Advances in Intelligent Systems Research, volume 165
International Conference on Modeling, Simulation, Optimization and Numerical Techniques (SMONT 2019)

Modeling and Simulation of Millimeter Wave Radiation Characteristics of Aquatic Vegetation

Shan Li , Guangfeng Zhang*, Qiang Shi, Li Zhu and Hong Wang
School of Electronic and Optical Engineering, Nanjing University of Science and Technology, Nanjing 210094, China
*Corresponding author

***Abstract*—The pollution of aquatic vegetation has become more and more serious in China. Based on the multi-layer medium model of aquatic vegetation and the growth characteristics of the aquatic vegetation, the radiant temperature of the aquatic vegetation is simulated as a function of the angle of incidence and as a function of time. Subsequently, in order to verify advantages of the millimeter wave radiometer in monitoring the growth of aquatic vegetation, measurement of the radiant temperature of aquatic vegetation by means of radiometer with vertical polarization, horizontal polarization and fixed angle of incidence sweeping. Based on modeling and simulation, we did experiments and found through experiments that the radiant temperature of aquatic vegetation is higher than the radiant temperature of the water surface. It shows that the radiometer can effectively distinguish between water surface and aquatic vegetation. The experimental data is consistent with the trend of the simulation results, indicating that the growth of aquatic vegetation can be monitored using the millimeter wave radiometer accurately.**

Keywords—aquatic vegetation; simulation; radiant characteristic modeling; radiometer; growth characteristics

I. INTRODUCTION

With the development of economy and industry, our living environment is facing many problems. Water pollution is the most significant one, and the massive reproduction of aquatic vegetation is one of the causes of water pollution. The millimeter wave radiometer has the characteristics of strong detection capability, strong anti-interference ability, high detection accuracy and no weather influence[1]. At present, the research on millimeter wave radiation at home and abroad mainly focuses on soil, ocean and moon soil [2-4], and there are relatively few studies on the monitoring of pollution and growth of surface plants, and lack of relevant data. At present, in the aspect of water pollution and surface plant monitoring, Cloete[5] used smart sensors to monitor water pollution in real time, Francesco Fornai[6] designed an automatic water pollution monitoring and sampling system for sensorized autonomous vehicles (ASVs), Guo Chenhua[7] proposed an accurate method for extracting potential risk source data from water pollution environment in view of the inaccurate results of risk source data classification and the long time used for data extraction in current risk source data extraction methods.

Based on the analysis of the radiant characteristics of the water surface and the characteristics of the water surface plants, the radiation temperature of the aquatic vegetation was simulated as a function of the incident angle and the curve with time, and the relevant experimental tests were carried out using an 8 mm band radiometer.

II. FUNDAMENTAL THEORIES

A. Brightness Temperature Model of The Water Surface

The brightness temperature of the smooth water surface is:

$$T_B(\theta; p) = \left[1 - \Gamma(\theta; p)\right] T_0 \tag{1}$$

In (1), θ is the angle of incidence, T_0 is the physical temperature of the water, $\Gamma(\theta; p)$ is the specular reflection coefficient and it's a function of the incident angle θ, the polarization mode p and the complex permittivity of water.

Assume the relative permeability of water bodies is μ_2 and μ_2 =1. The relative complex permittivity of water is ε_2 .So, we can get the specular reflection coefficient as,

$$\Gamma(\theta; h) = \left| \frac{cos\theta - \sqrt{\varepsilon_2 - \sin^2\theta}}{cos\theta + \sqrt{\varepsilon_2 - \sin^2\theta}} \right|^2 \tag{2}$$

$$\Gamma(\theta; v) = \left| \frac{\varepsilon_2 cos\theta - \sqrt{\varepsilon_2 - \sin^2\theta}}{\varepsilon_2 cos\theta + \sqrt{\varepsilon_2 - \sin^2\theta}} \right|^2 \tag{3}$$

Among them, h represents horizontal polarization and v represents vertical polarization.

B. Dick Radiometer

The block diagram of the Dick radiometer [8, 9]is shown in Figure 1.

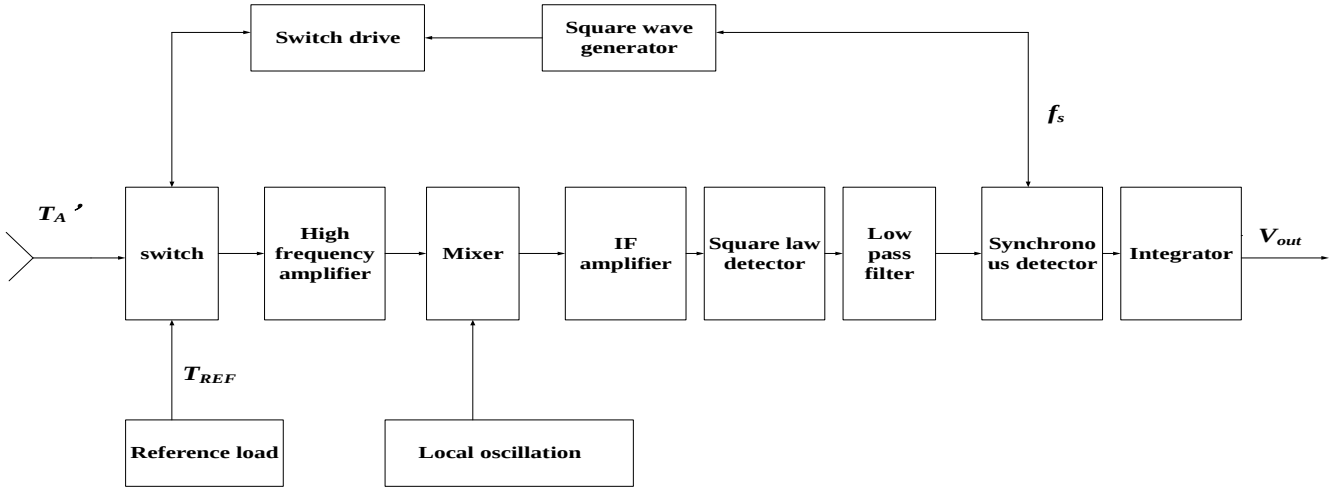

FIGURE I. BLOCK DIAGRAM OF DICK RADIOMETER

The switch turns the receiver on to the reference load and the antenna at the frequency of fs, so that in one cycle, the receiver receives thermal noise from the reference load for one half cycle, and the other half of the receiver receives thermal noise from the antenna, which shows that the receiver's input signal is modulated by the switch [10]. Therefore the output voltage of the antenna and the reference load is as follows,

$$V_d(t)=\begin{cases} V_{dREF}=\left(T_{REF}+T'_{REC}\right)kBG_S & 0\le t\le \tau s/2 \\ V_{dANT}=\left(T'_A+T'_{REC}\right)kBG_S & \tau s/2\le t\le \tau s \end{cases} \quad (4)$$

In (4), k is the Boltzmann constant, B is the system equivalent noise bandwidth before detection, T_{REF} is the noise temperature of the reference load, τ_s is a switching cycle, T'_A is the temperature of antenna, T'_{REC} is the temperature of equivalent input noise and Gs is the gain. So, the DC component of the output voltage after filtering noise is,

$$\overline{Vout}=\frac{1}{2}G_S\left[\left(T_{REF}+T'_{REC}\right)-\left(T'_A+T'_{REC}\right)\right] \quad (5)$$

The AC component in the output voltage V_{out} after filtering out noise is roughly composed of three parts, as shown below,

(1) Uncertainty caused by the gain fluctuation of the system itself

(2) Inaccuracy caused by the noise signal input from the radiometer when the reference load is switched on

(3) The uncertainty caused by the noise input from the radiometer when the antenna is switched on.

III. GROWTH CHARACTERISTICS SIMULATION

The excessive growth of aquatic vegetation caused by the eutrophication of water bodies has caused pollution of aquatic vegetation. Water plants generally include water hyacinth, cyanobacteria, green algae, water lily, leeks, water hyacinth, and so on. Aquatic vegetation like water hyacinth and cyanobacteria have strong vitality and rapid reproduction, and are prone to large-scale outbreaks. Therefore, it must be prevented in advance. For example, a water hyacinth can be propagated to 10-40 strains only in 30 days [11]. Now taking cyanobacteria as an example, the growth of cyanobacteria can have three stages. Take 30 days as an example, 1-10 days is the growth period, 11-20 days is the peak period of growth, and 21-30 days is the decline period of growth [12]. The growth curve of the simulated cyanobacteria is shown in Figure 2.

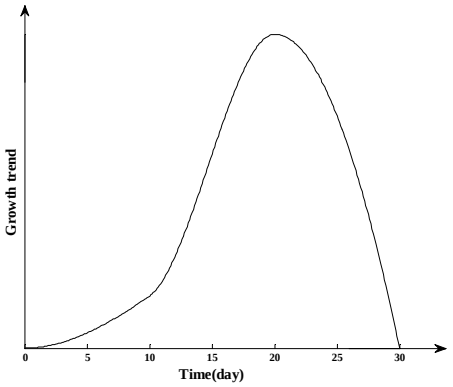

FIGURE II. CYANOBACTERIA GROWTH CURVE

As can be seen from Figure 2, when the cyanobacteria grow to the tenth day, mass reproduction begins and the growth rate begins to accelerate. Growth peaked on the twentieth day and growth slowed after twenty days .According to the Multi-layer media model based on aquatic vegetation [13]. T_B is the brightness temperature of the surface plants observed by the radiometer. The first layer of the aquatic vegetation, which is the total brightness temperature of the vegetation layer, can be expressed by (6).

$$T_B(\theta_1; p) = T_{B1}(\theta_1; p) + T_{L1}(\theta_1; p)$$
$$= \frac{1-\Gamma_1}{1-\Gamma_1\Gamma_2/L_2^2} \bullet \left(1+\frac{\Gamma_2}{L_2}\right) \bullet \left(1-\frac{1}{L_2}\right) T_{S2} + \quad (6)$$
$$\frac{1-\Gamma_1}{(1-\Gamma_1\Gamma_2/L_2^2)L_2} T_{H2}$$

In (6), p is the polarization of electromagnetic waves and θ_1 is the angle at which electromagnetic waves are incident on the first layer of vegetation. T_{B1} is the radiant brightness temperature of the first layer of vegetation, that is, the second layer of dielectric layer. T_{L1} is the superposition of the radiant temperatures of all the dielectric layers below the first layer of vegetation. Γ_i is the reflectivity of the i-th layer medium and the (i+1)th layer medium at their interface. T_{S2} is the amount of spontaneous radiation of the second dielectric layer of the surface plant. $T_{H,i-1}$ is composed of the i-th layer medium and all of the following dielectric layer radiation temperatures reaching the remaining values above the interface of the (i-1)th layer and the i-th layer.

Recursively, when i=N-1 and the Nth layer is the lowermost water body, assuming that the water body is infinitely deep, the radiation temperature emitted by the water body to the interface between the N-1 layer medium and the Nth layer water body is,

$$T_{H,N-1} = (1-\Gamma_{N-1})T_N \quad (7)$$

IV. RESULTS AND ANALYSIS

Based on the study of the growth characteristics of aquatic vegetation and the multi-layer medium model, the radiant temperature curve of the cyanobacteria was simulated Figure 3 is a radiant temperature diagram of cyanobacteria as a function of incident angle, and Figure 4 is a radiant temperature diagram of cyanobacteria as a function of time. In order to verify the advantages of millimeter-wave radiometers in aquatic vegetation pollution monitoring, experiments on the outdoor 8 mm band aquatic vegetation radiation characteristics were carried out in Zixia Lake. Comparing the experimental data with the simulated radiant temperature, the advantages of the millimeter wave radiometer in aquatic vegetation pollution monitoring were verified. Test location is Zixia Lake on campus. Environment temperature is 35.7 ° C and humidity is 44%. This experiment uses the overall calibration method for calibration. The test environment is shown in Figure 5.

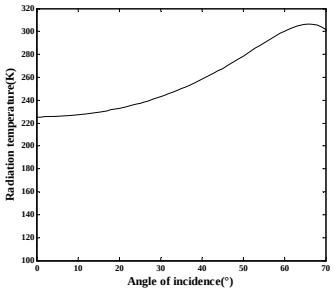

FIGURE III. BRIGHTNESS AND TEMPERATURE CURVE OF CYANOBACTERIA WITH INCIDENT ANGLE

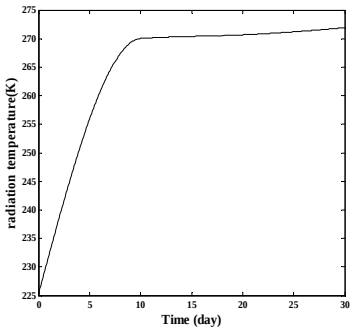

FIGURE IV. BRIGHTNESS AND TEMPERATURE CURVE OF CYANOBACTERIA OVER TIME

FIGURE V. LAB ENVIRONMENT

The experimental procedure is as follows: the 8 mm radiometer is placed at a height of 1.3 m from the ground, and the aquatic vegetation -water lily is used as the detection target. The angle between the main beam of the receiving antenna of the millimeter wave radiometer and the ground perpendicular is changed every ten degrees. And record the voltage value on the radiometer to get the radiation data of the water lily. Because of the limitations of the measurement environment, only the radiation temperature of the water lily with a pitch angle between 15 ° and 60 ° was measured. The radiant temperature curve of water lily is shown in Figure 6.

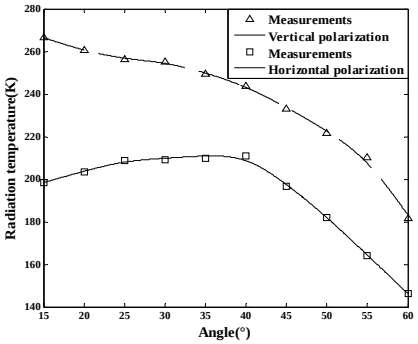

FIGURE VI. RADIANT TEMPERATURE CURVE OF WATER LILY

Through data analysis, we can find that,

(1) In the 8 mm band, the polarization of the water lily is not very obvious;

(2) The radiant temperature of the surface of the water lily gradually decreases with the gradual increase of temperature between 15° and 60°. This is because the distribution of water lily is relatively sparsely affected by the water surface background at 60°. Comparing Fig. 4 with Fig. 6, it can be seen that the radiant temperature changes of water lily and cyanobacteria are about the same. However, it may be affected by human factors and environmental constraints. The simulated radiant temperature curve of cyanobacteria is smoother than that of the water lily. In the experiment of measuring the radiation characteristics of water lily, an 8 mm radiometer was set up on the side of Zixia Lake in the school, and then the antenna handle was shaken to make the radiometer take an incident angle of 60°. Because of the limitation of the detection environment, the water lily can only be horizontally swept in the range of 0°-60°, and the corresponding radiation temperature is obtained. The specific measurement data obtained is shown in Table 1.

It can be seen from Table 1 that the radiometer antenna does not illuminate the water lily at 0°, the measured value of 0° should be the radiant temperature of the water surface. So it can be concluded that the radiant temperature of aquatic vegetation is higher than the radiant temperature of the water surface.

TABLE I. THE RADIATION TEMPERATURE CHANGES WITH THE HORIZONTAL SWEEP ANGLE WHEN THE INCIDENT ANGLE IS 60°

Angle(°)	0	10	20	30	40	50	60
Radiation temperature (K)	226.0	245.6	245.6	249.1	249.1	267.6	284.9

V. CONCLUSION

In this paper, the radiation characteristics of aquatic vegetation were studied by using 8 mm band radiometer. According to the growth characteristics and radiation characteristics of aquatic vegetation, the curve of radiant temperature of cyanobacteria or water lily with incident angle and the curve of brightness temperature of cyanobacteria or water lily with time were simulated and experiments were conducted on campus. The experimental and simulation results show that the 8 mm radiometer can effectively distinguish the water surface and the aquatic vegetation. We can draw a conclusion that the millimeter wave radiometer has advantages in the monitoring the growth and pollution of aquatic vegetation. But, due to the fact that the effects of spoiled cyanobacteria in the water were not considered in the simulation process, it is intended to be the focus of the research, and the research on the radiant temperature of aquatic vegetation with time is further studied and analyzed.

ACKNOWLEDGMENT

We gratefully acknowledge the financial support of National Natural Science Foundation (grant number 61371038) and Jiangsu Overseas Research & Training Program for University Prominent Young & Middle-aged Teachers and Presidents.

REFERENCES

[1] Hu Dongxiang, "Modeling and experimental study of millimeter wave radiation characteristics of water pollution," Nanjing: Nanjing University of Science and Technology, 2013.

[2] Yin X B, Liu Y G, Wang Z Z, "A new algorithm for microwave radiometer remo-tesening of sea surface salinity and temperature ," Science in China, Ser. D Earth Science-es, 51(11), 2006,pp.1368-1378

[3] Boyarskii D. A, Tik Honov V, Komarova N Y, "Model of Dielectric constant of bound water in soil for applications of microwave remote sensing ," Progress in Electromagnetic Research,(35), 2002 ,pp. 251-269.

[4] Lian Wei, Chen Shengbo, Meng Zhiguo, Zhang Feng, Zhang Ying, "Retrieving the dielectric constant of lunar soil based on the brightness data of the No.2 satellite microwave radiometer," Earth Science Journal of China University of Geosciences. 39(11),2014, pp. 1744-1750.

[5] Cloete N.A, Malekian R, Nair L, "Design of Smart Sensors for Real-Time Water Quality Monitoring," IEEE Access,(4),2016,pp.3975-3990.

[6] Francesco Fornai, Gabriele Ferri, Alessandro Manzi, Francesco Ciuchi, Francesco Bartaloni, "Cecilia Laschi. An Autonomous Water Monitoring and Sampling System for Small-Sized ASVs,".IEEE Journal of Oceanic Engineering, 42(1),2017, pp.5-12.

[7] Guo Chenhua, Zhang Dengrong, Lu Jinxia, "Simulation of accurate extraction method of potential risk source data for water pollution environment ," Computer Simulation, 35(10),2018, pp. 436-439.

[8] Zhang Zuyin, Lin Shijie, "Microwave radiation measurement technology and application,". Beijing: Publishing House of Electronics Industry, 1995, pp.62-64.

[9] Yan Jinhai, Li Xingguo, Wang Min, "Research on Detection of Helicopter by Millimeter Wave Radiometer," Journal of Detection & Control, 23(4),2001, pp.37-40.

[10] Guo Lei, "Research on focal plane imaging method and system simulation ," University of Electronic Science and Technology of China, 2009.

[11] Duan Hui, Qiang Sheng, Wu Hairong, Lin Jincheng,"Water Hyacinth [Eichhornia crassipes (Mart.) Solms.] ," Weed Science, (02),2003,pp.40-41.

[12] Kong Fanxiang, Ma Ronghua, Gao Junfeng, Wu Xiaodong,"Theory and Practice of Prevention, Prediction and Early Warning of Cyanobacteria Bloom in Taihu Lake,"vJournal of Lake Science,21(03),2009,pp.314-328.

[13] Li Beibei, Zhang Guangfeng, Yan Guowei, Zhou Yanyan, Liu Jing,"Surface vegetation detection method based on millimeter wave radiation characteristics,".Computer Measurement & Control, 24(07), 2016, pp.45-48